Social isolation modulates appetite and defensive behavior via a common oxytocinergic circuit in larval zebrafish

Caroline L. Wee[1,2,3§], **Erin Song**[1§], **Maxim Nikitchenko**[1,4§], Sandy Wong[1], Florian Engert[1]*, Samuel Kunes[1]*

[§]Equal-contribution first authors
*Corresponding authors

Affiliations:
[1]Department of Molecular and Cellular Biology and Center for Brain Science, Harvard University, Cambridge, Massachusetts, USA
[2]Program in Neuroscience, Department of Neurobiology, Harvard Medical School, Boston, Massachusetts, USA
[3]Present address: Institute of Molecular and Cell Biology, A*STAR, Singapore
[4]Present address: Duke University, Durham, North Carolina, USA

Correspondence:
Florian Engert / Samuel Kunes
Department of Molecular and Cellular Biology
Harvard University, 16 Divinity Ave, Biolabs 2073
Cambridge, MA 02138, USA

ABSTRACT
How brains encode social stimuli and transform these representations into advantageous behavioral responses is not well-understood. Here, we show that social isolation activates an oxytocinergic, nociceptive circuit in the larval zebrafish hypothalamus. We further demonstrate that chemical cues released from conspecific animals modulate its activity to regulate defensive behaviors and appetite. Our collective data reveals a model through which social stimuli can be integrated into fundamental neural circuits to mediate adaptive behaviour.

INTRODUCTION

In mammals, signaling in oxytocinergic (OXT) circuits modulates a wide spectrum of socially driven behaviors, ranging from pair bonding and parental care to the responses to stress and pain[1–3]. OXT has also been described as a potent regulator of appetite[4,5]. We reported recently that the larval zebrafish OXT circuit encodes a response to aversive, particularly noxious stimuli and directly drives nocifensive behavior via brainstem premotor targets[6]. Moreover, studies in both zebrafish[6–8] and mammals[9,10] suggest that the OXT-expressing neuronal population is anatomically and functionally diverse, and might also modulate multiple behaviors in zebrafish. Here, in a brain-wide screen[11] for neuronal populations whose activity reflects social context, we show that larval zebrafish oxytocinergic circuits display diverse responses to conspecific chemosensory stimuli, and are key effectors for social context modulation of nociceptive and appetite-driven behaviors. Our results reveal a simple algorithm by which neuromodulatory neurons can represent social context to exert flexible control over hard-wired behavioral drives.

RESULTS

Brain-wide activity mapping of social isolation and its rescue by conspecific chemical cues

Using pERK based whole-brain activity mapping (MAP-Mapping[11]), neural activity in brains of briefly (2 hrs) socially-isolated larvae (7 - 8 **d**ays-**p**ost-**f**ertilization; dpf) was compared to animals that had been maintained in the presence of similarly-aged conspecifics. We found that isolated fish showed an enhancement of neural activity in specific regions, including the telencephalon (especially subpallium), hindbrain, locus coeruleus, area postrema, caudal hypothalamus, preoptic area (PO, homolog of the hypothalamic paraventricular nucleus in mammals) and posterior tuberculum (PT) (Fig. 1a-b, Supplementary Movie 1, Supplementary Data 1). Many of these same regions are activated by noxious or aversive stimuli[6,7]; they may thus represent the signature activity pattern of a negative internal state, which can be similarly triggered by social deprivation. Neurons expressing the peptide oxytocin (OXT) are abundant in the PO and PT[6,12,13] regions, and as we describe below, OXT-positive neuron clusters in both of these areas (OXT_{PO} and OXT_{PT} respectively) display greater activity in socially-isolated fish. To acquire a more precise quantitation of OXT activity in relation to the social environment, we measured pERK activity for individual GFP-labeled OXT neurons (*Tg(oxt:GFP)*), as well as surrounding non-OXT PO and PT neurons, in high resolution confocal microscopic images of dissected brains[6] (Fig. 1c-d, Supplementary Fig. 1). We found that a subset of both OXT neurons and surrounding non-OXT neurons were significantly more active in socially-isolated fish, as was recently observed in the context of noxious stimuli[6] (Fig. 1a-b). Thus, the OXT

population might encode negative valence stimuli, such as the environmental stimulus of social isolation.

FIGURE 1

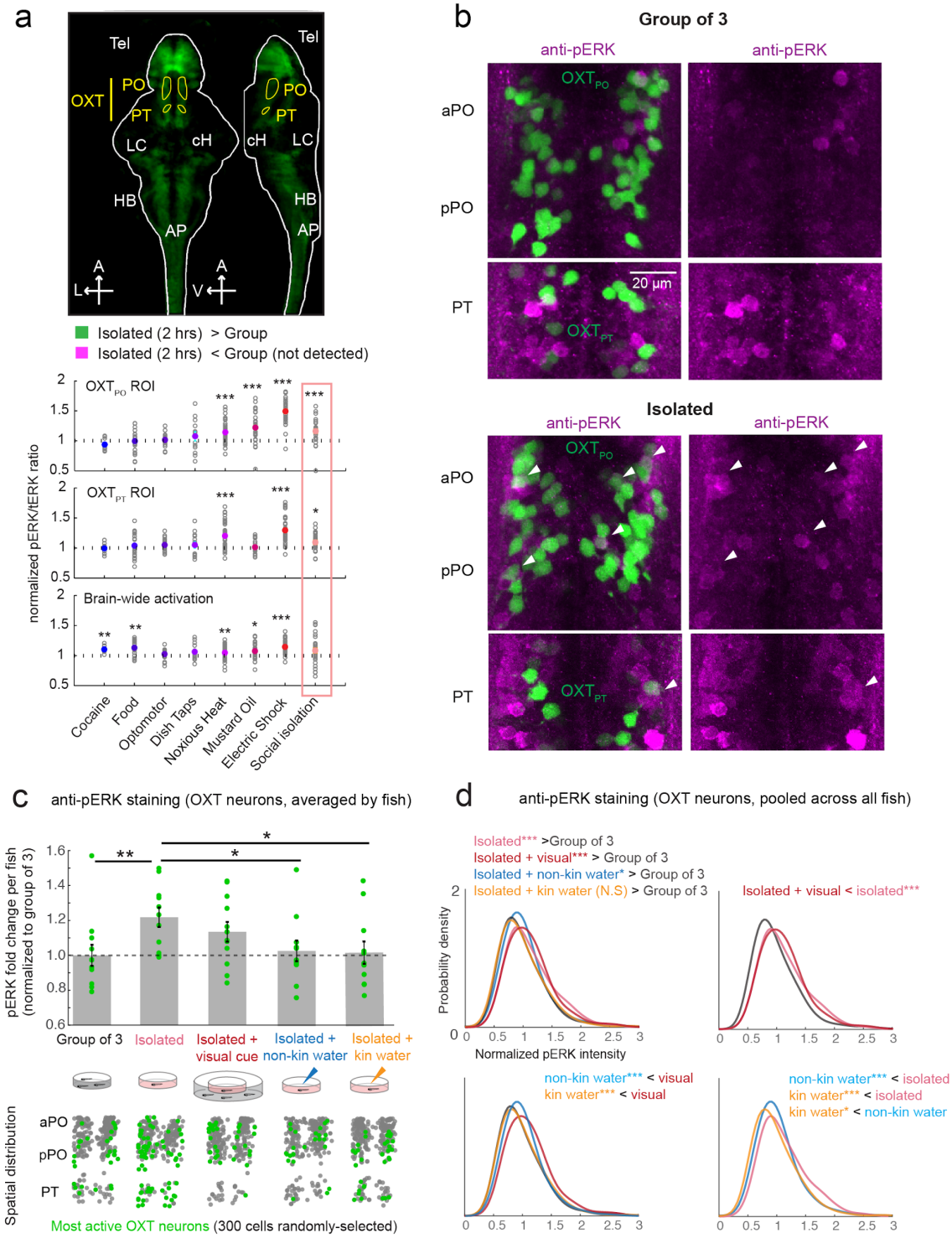

Figure 1: phospho-ERK based mapping reveals OXT neuron modulation by social context

(a) Top: pERK-based activity mapping to compare brain activity of isolated vs. social fish. Green voxels highlight regions that are significantly more active in isolated fish as compared to fish maintained in groups. This final map was generated by averaging data from 5 independent experiments in which isolated fish are compared to fish kept in groups of 3 (2 experiments), 5 (1 experiment) or 10 (2 experiments) (See **Supplementary Movie 1**; FDR Threshold used = 0.05%. Yellow = Outline of preoptic (OXT_{PO}) and posterior (OXT_{PT}) oxytocin populations). These masks were used for the quantification of activity in **bottom**. Other ROIs are quantified in **Supplementary Data 1.** Tel = Telencephalon, cH = Caudal Hypothalamus, LC = Locus Coeruleus, AP = Area Postrema, HB = Hindbrain.
Bottom: Social isolation significantly activates OXT-expressing brain regions. Here, the mean pERK signal was calculated per fish across the specified ROIs. Data for other stimuli was also included in Wee et al (2019)[6]. Adjusted p values for social isolation: ***p = 0.00084 (OXT_{PO}), *p = 0.03 (OXT_{PT}), 0.42 (whole brain). Wilcoxon signed-rank test relative to a median of 1, Bonferroni correction.

(b) High-resolution imaging of pERK expression in OXT neurons in brains from dissected isolated fish **(bottom),** compared to the brains of fish kept in groups of 3 **(top)**. Maximum intensity projection of one fish from each condition are shown (green = preoptic (OXT_{PO}) and posterior (OXT_{PT}) oxt:GFP-positive neurons, magenta = anti-pERK staining). White arrows indicate OXT neurons with high pERK intensities. Scale bar = 20 µm.

(c) Top: Effect of social isolation and social sensory cues on mean OXT (PO + PT combined, green) neuron activity per fish. pERK intensities of individual OXT and non-OXT (see **Supplementary Fig. 1**) cells were extracted automatedly as reported in Wee et al (2019)[6]. pERK intensities shown are normalized to those of control fish (i.e. fish maintained in groups of 3). Social isolation induced a 1.2 fold increase in OXT neuron pERK activity relative to fish maintained in groups of 3. Visual cues of conspecifics moderately reduced OXT neuron pERK activity (1.1 fold relative to group), non-kin and kin water cues induced an even stronger reduction in OXT neuron pERK activity (1.01 and 1.00 fold relative to group). OXT neurons: p= 0.0074** (group vs isolated) / 0.069 (group vs visual) / 0.52 (group vs non-kin water) / 0.83 (group vs kin water) / 0.37 (isolated vs visual) / 0.022* (isolated vs non-kin water) / 0.036* (isolated vs kin water) / 0. 21 (visual vs non-kin water) / 0.19 (visual vs kin water) / 0.65 (kin vs non-kin water). **Bottom:** Spatial distribution of the most active OXT-positive neurons. Active neurons were defined using a pERK intensity threshold above which only 10% of neurons are active in the control (i.e group of 3) condition. 300 OXT cells were randomly sampled across all fish.

(d) Probability distributions (kernel density estimate (KDE)) of normalized pERK fluorescence across all neurons per group. Multiple panels are shown to aid visualization. Fish were either kept in groups of 3 (gray, n = 993 neurons from 12 fish), isolated (pink, n = 931 neurons from 11 fish), isolated but exposed to visual cues of conspecifics through a transparent barrier (red, n = 902 neurons from 12 fish) or isolated but exposed to non-kin-conditioned water (blue, n = 866 neurons from 11 fish) or kin-conditioned water (orange, n= 856 neurons from 12 fish). Isolated fish had significantly higher OXT neuron pERK activation than fish in a group (***p = 2.6×10^{-35}). Isolated fish presented with visual conspecific or non-kin water cues also had significantly higher OXT pERK activity than fish in a group (***p = 4.8×10^{-15} and *p = 0.027 respectively), whereas kin water did not significantly change OXT neuron activity relative to fish in group (p = 0.67). All cue types significantly reduced OXT neuron activity relative to isolated fish (***2.8×10^{-6} (visual), ***6.3×10^{-26} (non-kin), ***2.0×10^{-34} (kin)). Kin water induced significantly-lower OXT neuron activity relative to non-kin water (*p = 0.012). Both kin and non-kin water reduced OXT neuron activity significantly more than visual cues (***p = 2.9×10^{-15} and ***p = 2.6×10^{-9} respectively), two-sided Wilcoxon rank-sum test.

123 As a step toward elucidating the nature of the social signal, we compared OXT neuronal
124 activity in animals exposed to the separated visual or chemical cues of a social environment.
125 We find that water conditioned by prior exposure to conspecific larval fish (see Methods)
126 reduced the elevated OXT neuronal activity observed in socially isolated fish, whereas visual
127 exposure to conspecific larval fish (maintained in a separate water enclosure) had minimal
128 effect (Fig. 1c-d). We also examined the effect of water conditioned with similarly-aged sibling
129 (kin) fish in relation to similarly-aged fish of a different strain background (non-kin). Both 'kin'
130 and 'non-kin' conditioned water was sufficient to reduce OXT neuron activity (Fig. 1c-d), but the
131 effect of kin water was significantly stronger (Fig. 1d). Nearby OXT-negative neurons in the PO
132 and PT area were also suppressed by conspecific-conditioned cues (Supplementary Fig. 1).
133 Thus OXT and PO/PT neural activity in larval zebrafish is increased during brief (2 hr) social
134 isolation, and this activity is equivalently (and rapidly, see Fig. 2) suppressed by exposure to
135 water that had held conspecific larval fish.
136
137 *In vivo calcium imaging reveals diverse olfactory and OXT neuronal responses to chemical*
138 *conspecific cues*
139 We next turned to *in vivo* calcium imaging to acquire a temporally precise record of OXT
140 neuronal activity. Imaging was performed on larvae in which *UAS:GCaMP6s* was driven directly
141 in OXT neurons with an *oxt:Gal4* driver (Fig. 2a). Tethered 8-11 dpf fish were subjected to either
142 conditioned or control water released in 10 second pulses. We show that pure water flow, which
143 represents a mechanosensory stimulus, mildly activated OXT neurons, whereas water that had
144 been conditioned by prior incubation with larval fish triggered an immediate relative reduction of
145 OXT neuronal activity (Fig. 2a,e-f). We next tested whether OXT neuron calcium activity also
146 discriminates between kin and non-kin conspecific cues[14,15]. To that end, OXT neuronal
147 activity was compared between sibling-conditioned water (kin water') and water conditioned by
148 larvae of a distinct genetic background[16] ('non-kin water'). We also examined water conditioned
149 by the presence of adult kin, which is potentially an aversive predator cue, as adult zebrafish
150 consume their own young. To minimize the effects of familiarity, conspecifics used to generate
151 conditioned cues were raised apart (in a different dish) from experimental fish.
152 Since water-borne chemical cues likely act as odorants, we included the olfactory bulb
153 (OB) in the areas specifically interrogated for changes in neuronal activity upon exposure to
154 these cues. When examined via labeling with the pan-neuronal GCaMP line *HuC:GCaMP6s*
155 (Fig. 2a-d, Supplementary Fig. 2), each of the three conditioned water types (kin, non-kin and
156 adult kin) generated overlapping but distinct activity signatures within the OB and OXT

populations (Fig. 2). As expected, kin water led to a relative reduction of the OXT neuron response (Fig. 2e-f). Adult water, on the other hand, led to a net increase in OXT activity with longer lasting dynamics, correlating with similarly longer lasting olfactory responses (Fig. 2c, e-f). Notably, non-kin water was less effective in reducing OXT neuron activity than kin water, and it elicited much weaker OB activity (Fig. 2f, also compare Fig. 2b to 2e), suggesting some subtle differences between kin and non-kin water effects that had also been observed with pERK imaging (compare with Fig. 1d).

FIGURE 2

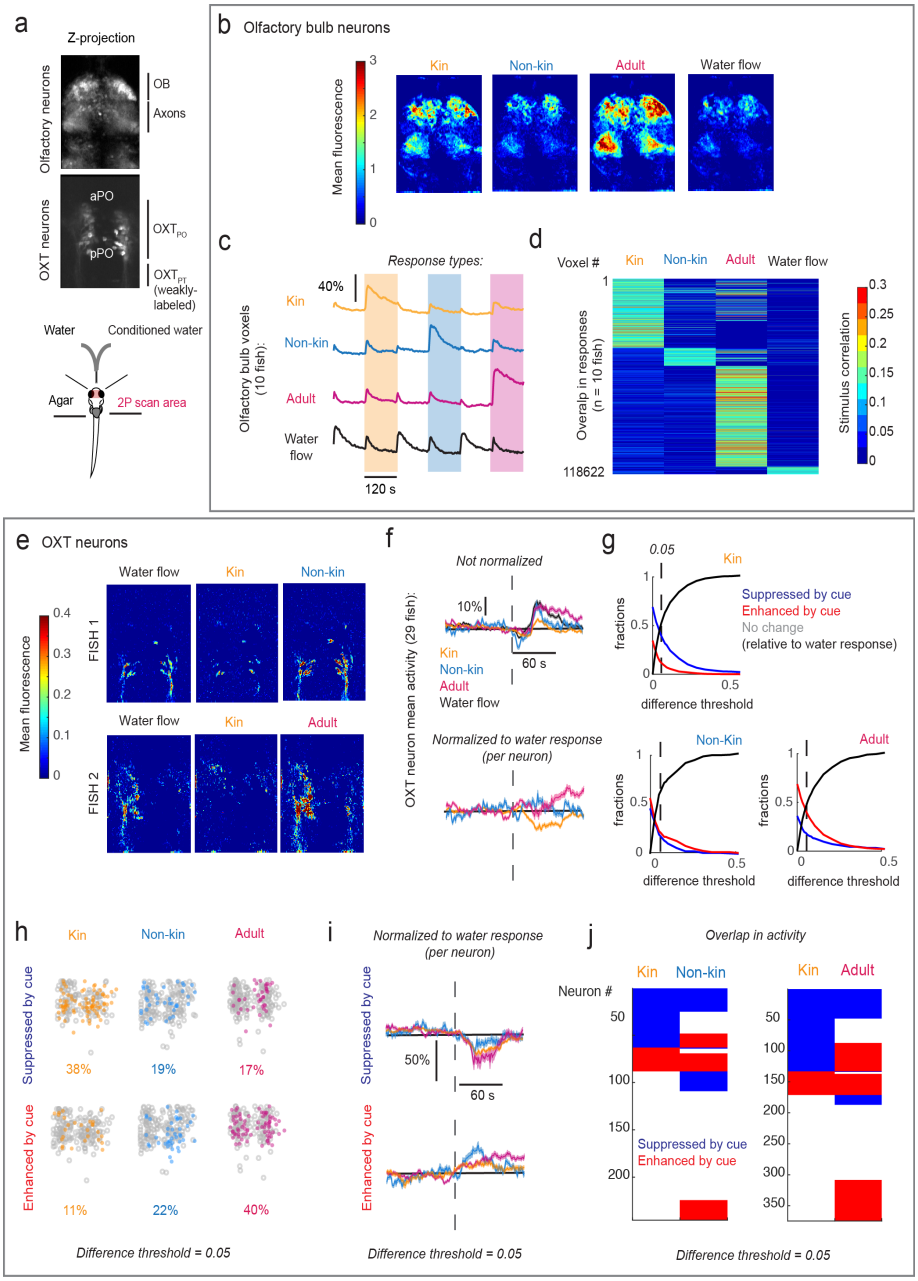

Figure 2: Calcium imaging confirms OXT neuron modulation by conspecific cues

(a) Top: Z-projection of volumetrically-scanned brain regions (olfactory bulb and oxytocin neurons). The olfactory bulb was labeled using *Tg(HuC:GCaMP6s)*. The *Tg(oxt:Gal4; UAS:GCaMP6s)* transgenic line labels OXT_{PO} neurons strongly, with weaker labeling of the OXT_{PT} cluster. We did not image both regions simultaneously. **Bottom:** Schematic of imaging and cue delivery setup.

(b-d) Olfactory Bulb (OB) Imaging

(b) Mean OB fluorescence in response to different stimuli (kin, non-kin, adult or water flow) integrated over a 60 s period post-stimulus from a single fish. See **Supplementary Fig. 2** for more examples.

(c) Mean stimulus-triggered calcium responses from 10 fish. All four stimuli (kin, non-kin, adult or water flow) were presented to each fish. Each plot is the average calcium trace of all OB voxels that are selective for one of the four stimuli. On average, about 5/1.5/10/1% of voxels (n=17856/5357/34672/3522 out of 345688 total voxels) were specific to kin, non-kin, adult conditioned water and water respectively. Olfactory responses are sustained and decay slowly throughout the imaging interval (2 min).

(d) Quantification of overlap of OB responses to different stimuli (118622 voxels that are responsive (r>0.1) to at least one of the stimuli, aggregated across 10 fish). While many voxels showed specific activation by individual stimuli, there were some overlapping responses between the cues. Color map indicates Pearson's correlation coefficient (r-value).

(e-j) OXT neuron imaging

(e) Mean OXT neuron fluorescence integrated over a 60 s period post-stimulus from two different fish, one imaged with kin and non-kin water, and another with kin and adult water.

(f) Top: Mean stimulus-triggered calcium responses of OXT neurons. All fish (29 fish, n=1033 neurons) were imaged with water or kin water, some additionally were imaged with either non-kin (8 fish, n =245 neurons) or adult water (10 fish, n = 374 neurons). **Bottom:** Mean stimulus-triggered calcium responses of each neuron normalized to its own mean water response. Gray broken line indicates stimulus onset. Shading indicates SEM.

(g) Fraction of OXT neurons that would be classified as suppressed (blue) or activated (red) by each water-borne cue, as a function of the mean difference in integrated calcium activity from the water response (i.e. difference threshold). A threshold of 0.05 (i.e. 5% difference) was used in subsequent panels.

(h) Spatial distribution and percentages of neurons that show either suppressed (**top**) or enhanced (**bottom**) responses to each cue relative to water. For accurate comparison of spatial distribution, 200 neurons were randomly selected from each group. Percentages are calculated based on a difference threshold of 0.05. Kin cues induced the highest percentage suppression (38%) and lowest percentage activation (11%), whereas adult cues induced the lowest percentage suppression (17%) and highest percentage activation (40%) of OXT neurons.

(i) Mean stimulus-triggered calcium responses of neurons classified as being suppressed (top) or enhanced (bottom) by each cue, normalized to their mean water response. Shading indicates SEM.

(j) Visualization of overlapping OXT neuron representations between conspecific cues. Left: overlap between kin and non-kin water. Right: overlap between kin and adult water. We did not image all 3 cues

simultaneously. Red = enhancement, Blue = suppression, White = no change, based on difference threshold of 0.05. Approximately one third of neurons suppressed by kin water were also suppressed by non-kin (40%) and by adult water (36%). In addition, a common subset of neurons activated by kin water were also activated by non-kin (76%) and adult (90%) water. However, 24% and 35% of kin water-suppressed neurons were alternatively activated by non-kin and adult-conditioned water, respectively.

OXT neurons are diverse in their circuit connectivity[8,17–19] and responses to social deprivation (Fig. 1) and nociceptive input[6]. To further resolve this heterogeneity, we used calcium imaging to classify individual OXT neurons into populations that either reduce or increase their activity in response to water-borne conspecific cues. We found that, across a range of thresholds, the fraction of OXT-positive neurons whose activities were suppressed by larval kin-conditioned water was consistently higher than the fraction of neurons that were activated (Fig. 2g). Non-kin-conditioned water, in contrast, induced equivalent neuronal fractions with increased or suppressed activities. Water conditioned by adult fish triggered a greater fraction of neurons with enhanced activity (Fig. 2g). Under all conditions, activated or suppressed neurons were spatially distributed throughout the OXT-positive PO and PT domains, instead of being segregated into distinct areas (Fig. 2h-i). Further, the specific response properties of individual neurons to one conspecific cue did not predict strongly how they would respond to alternate cues, although we observed that kin water-activated OXT neurons tended to also be commonly activated by other conspecific (non-kin or adult) cues (Fig 2j). The heterogeneity of the population suggests that OXT neurons as a group are able to differentially encode these stimuli and provide a basis to discriminate between them in affecting behavior.

Conspecific cues suppress nociceptive OXT circuits and defensive behavior

Social buffering is a widely-observed phenomenon in which the presence of conspecifics ameliorates the effects of aversive experience[20,21]. We previously showed that a large fraction of OXT neurons are activated by noxious stimuli and drive defensive behaviors, specifically through brainstem premotor targets that trigger vigorous large-angle tail bends[6]. Given that most of the OXT circuitry appears to be suppressed by water-borne social cues derived from closely-related conspecifics, we posited that these cues might reduce the nocifensive behavior induced by the stimulation of TRPA1 receptors. Indeed, increased swim speed triggered by nociceptive TRPA1 receptor activation was significantly ameliorated by the presence of kin-conditioned water (Supplementary Fig. 3). Consistent with the idea that this reduced nocifensive response involves the suppression of OXT neurons, kin water significantly also reduced the peak tail angles of responses to TRPA1 stimulation in tethered fish (**$p = 0.0081$, $n = 16$ fish, Fig. 3a-b).

252 **FIGURE 3**

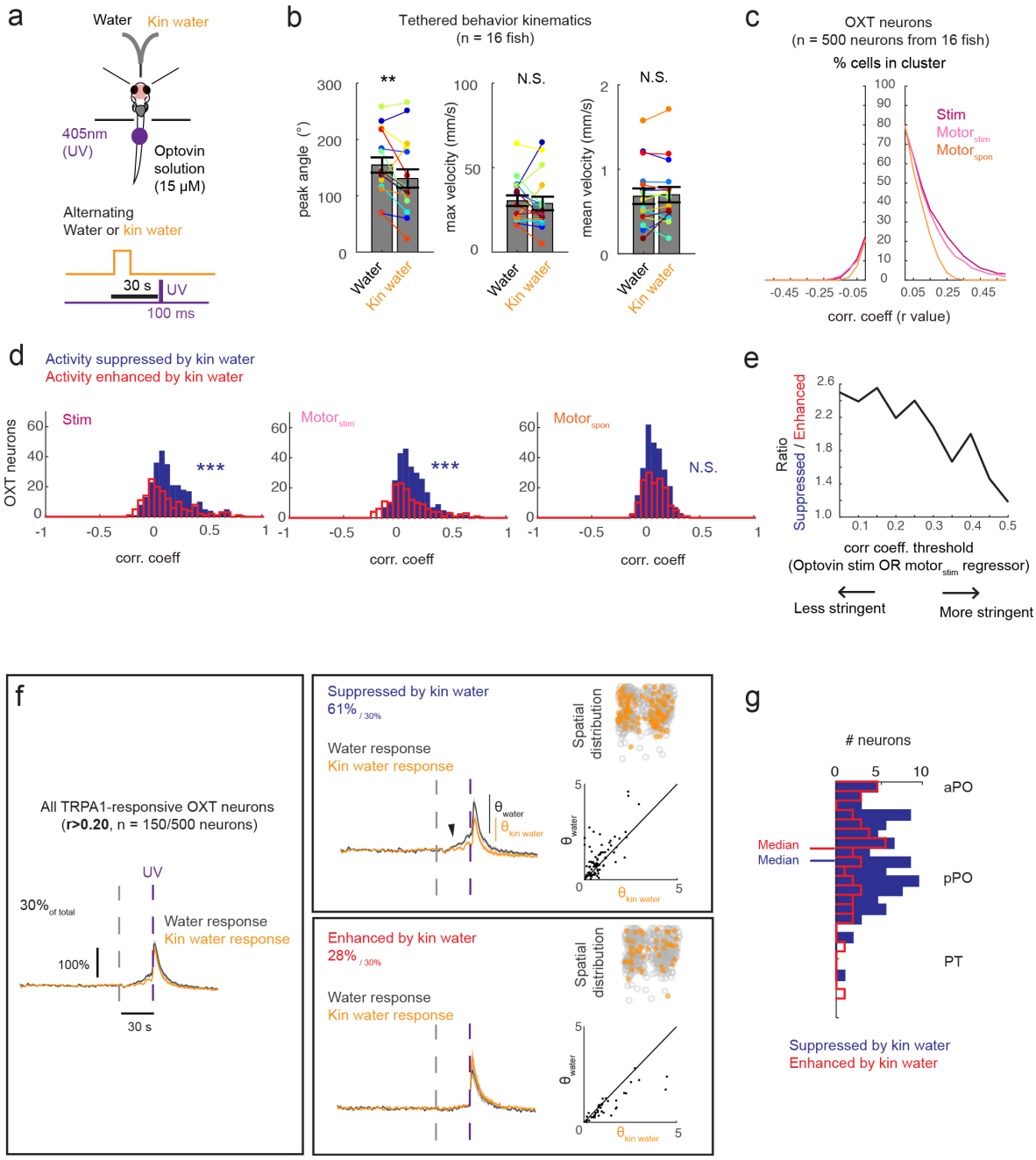

253

254 **Figure 3: Chemical kin cues modulate OXT nociceptive responses and defensive behavior**

255

256 **(a)** Top: Schematic showing setup to probe effect of conspecific-conditioned water on TRPA1-induced
257 nocifensive responses. Bottom: Fish were tethered with their nose/mouth and tails freed, and incubated in
258 15 μM Optovin solution. Alternating pulses of water or conspecific water were presented, followed by a
259 100 ms pulse of UV light after 30 s to activate TRPA1 receptors.

260

(b) Kin water significantly reduced the mean peak tail angle (**p =0.0081) of TRPA1-induced tail bends. Maximum and mean velocity was not significantly changed (p = 0.18 and 0.63). One-sided Wilcoxon signed-rank test, n = 16 fish.

(c) The calcium trace of each OXT neuron was cross-correlated with stimulus regressors or motor regressors either within 5 s of TRPA1 stimulation ($motor_{stim}$), or outside of the post-stimulus window ($motor_{spon}$), as in Wee et al (2019)[6]. Panel shows percentage of OXT cells that will be classified as stimulus, $motor_{stim}$ or $motor_{spon}$-correlated as a function of Pearson's correlation coefficient threshold (r-value).

(d) Distribution of OXT neurons that are either suppressed (blue) or enhanced (red) by kin water, as a function of their Pearson's correlation coefficient with the stimulus, $motor_{stim}$ or $motor_{spon}$ regressors. Neurons that show kin water-induced suppression are significantly more correlated to TRPA1 motor and stimulus regressors (***$p = 7.2x10^{-5}$ (stim), ***$p = 9.3x10^{-5}$ ($motor_{stim}$), but not spontaneous movement regressors (p = 0.35).

(**e)** As the threshold for correlation with stim or $motor_{stim}$ regressors is relaxed (i.e. approaching smaller values), a larger proportion of suppressed rather than activated neurons are observed, suggesting that moderately TRPA1-responsive neurons are most strongly suppressed by kin water. As in **Fig. 2**, a difference threshold of 0.05 (i.e. 5%) was the cutoff for determining if responses were enhanced or suppressed by kin water.

(f) Left panel: Mean stimulus-triggered calcium responses of all TRPA1-responsive neurons in the presence of water (black) or kin-conditioned water (orange)**,** as a function of a medium stim or $motor_{stim}$ regressor coefficient threshold (r = 0.20) used to identify these neurons. See **Supplementary Fig. 4** for plots using other r-value thresholds. Shading indicates SEM. Gray dashed line = water or kin water delivery, Purple dashed line = UV stimulus onset. **Right panels:** Mean stimulus-triggered calcium responses for all TRPA1-activated neurons that are suppressed **(top)** or activated **(bottom)** by kin water, again for threshold of r = 0.20. n = 151 neurons (all TRPA1 activated) / 92 neurons (61%, suppressed by kin water) / 42 neurons (28%, activated by kin water) for both control and kin water conditions. **Top inset** shows the spatial distribution of these neurons. All neurons (n=500) are displayed. **Bottom inset** compares the magnitude (θ) of calcium fluorescence (Δf/f) change before and after TRPA1 stimulation for neurons that were identified to be suppressed or activated by kin water. Despite the differences in baseline activity that are induced by water flow (**see black arrow**) the magnitude of calcium fluorescence change post-TRPA1 stimulation is still modulated by kin water.

(g) Distribution along the A-P axis of suppressed and enhanced neurons (r>0.20).

To further tie nociceptive responses to social modulation of OXT neurons, we examined the effect of conspecific cues on the subset of OXT neurons that respond to TRPA1 stimulation. As we had previously done[6], each neuron's calcium activity was correlated with stimulus and motor regressors (Fig. 3c). For motor regressors, we further classified responses into those that occured within 5 s of the stimulus ($motor_{stim}$) or at other time points in the experiment ($motor_{spon}$). Individual OXT neurons were then subsequently grouped according to whether they displayed suppressed or enhanced TRPA1 responses following kin water presentation. We found that kin

307 water-suppressed neurons had significantly higher (right-shifted on the graph shown in Fig. 3d)
308 correlations with TRPA1 stimulus and $motor_{stim}$ regressors. Indeed, among OXT neurons that
309 had high TRPA1 responsiveness ($r > 0.35$; 13% of OXT neurons), a larger fraction of neurons
310 were suppressed (55%) rather than activated (33%) by kin water (Supplementary Fig. 4).
311 However, when *less stringent* criteria was used to define TRPA1 responsiveness (e.g. r
312 > 0.20, Fig 3f), the ratio of kin water-suppressed to kin water-activated OXT neurons increased
313 even further (Fig. 3d-e, also see Supplementary Fig. 4), indicating that the bulk of kin water-
314 suppressed OXT neurons are only moderately-responsive to TRPA1. When we included these
315 moderately-responsive OXT neurons in our analysis, we observed a clear divergence from
316 baseline activity *before* TRPA1 activation, which was induced by water flow alone (Fig. 3f, top
317 right panel), suggesting that these kin water-suppressed OXT neurons had *both* a water flow-
318 induced and TRPA1-specific response. Thus many kin water-suppressed OXT neurons are not
319 only responsive to TRPA1 stimulation, but also to other potentially aversive stimuli such as
320 water flow.
321 Notably, kin water was sufficient to reduce responses to *both* water flow *and* TRPA1
322 stimuli (even when accounting for baseline differences; Fig. 3f, top right panel). Further, these
323 kin water-suppressed neurons also tended to be more posteriorly-distributed, consistent with the
324 idea that they correspond to parvocellular, hindbrain-projecting neurons which drive motor
325 output[6] (Fig. 3g). In contrast, OXT neurons that showed enhanced activation under exposure to
326 kin water were more highly-selective for TRPA1 activation, and did not show apparent
327 responses to water flow (Fig. 3f, bottom right panel). Thus, the reduced nocifensive responses
328 of larval fish observed in the presence of social cues is directly reflected in the suppressed
329 activity of a subset of TRPA1-responsive neurons within the OXT circuit.
330
331 *OXT neuronal activity suppresses appetite in a conspecific cue-dependent manner*
332 In mammals, social isolation is associated not only with increases in aversive behavior, but also
333 with a reduction in positive-valence behaviors such as feeding[22]. To determine if this is also the
334 case in larval zebrafish, we first made use of an established and quantitative food intake assay
335 that measures gut fluorescence intensity caused by the ingestion of fluorescently-labeled
336 paramecia[23–25] (Fig. 4a). In this assay, larval fish were food deprived for a period of two hours to
337 increase appetite[23–25], either in isolation or in the presence of conspecific fish (Fig. 4a).
338 Subsequently, animals maintained under either of these two conditions were presented with
339 large excess of fluorescently labeled paramecia. Notably, fish maintained in isolation consumed
340 significantly less paramecia (i.e. food) than those kept in small groups. Additionally, when group

size was varied from 2 to 5 individuals, food intake per capita was observed to scale with group size (Fig. 4b). Finally, we observed that water-borne cues from closely related larval fish (kin fish), but not visual cues, were sufficient to rescue the isolation-induced suppression of food intake (Fig. 4c).

FIGURE 4

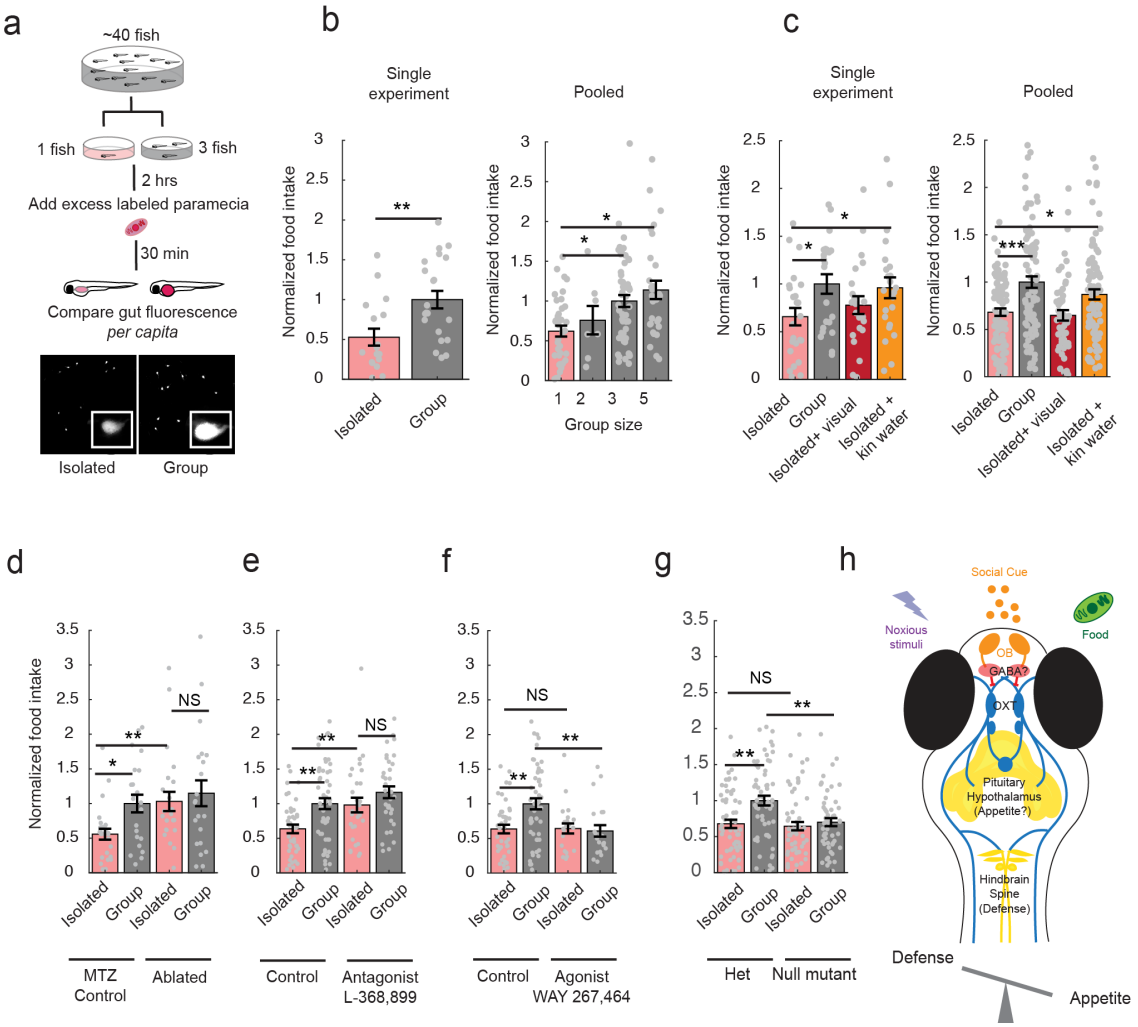

Figure 4: Manipulation of OXT signaling affects appetite in a social-context dependent manner

(a) Schematic of social behavior experiments. Larval zebrafish were raised in a group up to 7 or 8 dpf. They were then either isolated in a small dish or into a small group of 3 fish. After 2 hrs, fluorescently-labeled paramecia was added for 30 min, following which fish were fixed and subsequently imaged. Example raw fluorescence images are shown, with inset showing higher (100x) magnification image. Integrated gut fluorescence (area x intensity) was used to approximate food intake.

(b) Left: Gut fluorescence quantification from a single experiment demonstrates that isolated fish on average eat less, per capita, than fish in a group of 3. All gut fluorescence measurements are normalized to the mean food intake of fish in a group (**p = 0.0058, n = 21/17 fish, two-sided Wilcoxon rank-sum

359 test). **Right:** Normalized food intake (i.e. gut fluorescence normalized to the average gut fluorescence of
360 fish in a group of 3) scales with group size (n = 36, 7, 52, 29 fish, single asterisks depict p<0.05 using
361 one-way ANOVA corrected for multiple comparisons).
362
363 **(c) Left:** Chemical but not visual cues were sufficient to rescue isolation-induced feeding suppression in
364 a single experiment. *p = 0.03 (single vs group), *p = 0.04 (single vs kin water), p = 0.17 (single vs visual),
365 n = 24/24/22/23 fish, two-sided Wilcoxon rank-sum test. **Right:** Average of multiple experiments. p =
366 ***2.8283×10^{-4} (single vs group), *p = 0.02 (single vs kin water), p = 0.35 (single vs visual), n =
367 86/86/55/87, Wilcoxon rank-sum test.
368
369 **(d)** Cell-specific chemical ablation of OXT neurons specifically rescues effect of social isolation on
370 appetite (n = 65/59/57/56 fish). *p = 0.015 (single vs group), **p = 0.0017 (single control vs single
371 ablated), p = 0.76 (single ablated vs group ablated), two-sided Wilcoxon rank-sum test. Controls are
372 metronidazole (MTZ)-treated, non-transgene-expressing siblings.
373
374 **(e)** Oxytocin antagonist L-368,899 rescues isolation-induced suppression of food intake without
375 significantly changing food intake in a group (n=40/50/29/34 fish). **p = 0.0022 (single vs group), **p =
376 0.0091 (single control vs single antagonist), p = 0.09 (single antagonist vs group antagonist), two-sided
377 Wilcoxon rank-sum test.
378
379 **(f)** Oxytocin agonist WAY267,484 suppresses food intake in groups but does not affect food intake in
380 isolated fish (n=40/50/20/21 fish). **p = 0.0022 (single vs group), p = 1 (single control vs single agonist),
381 **p = 0.0069 (group control vs group agonist), two-sided Wilcoxon rank-sum test. Control groups for both
382 **(e)** and **(f)** are the same sets of fish, split up for better visualization. All data is from multiple sets of
383 experiments and normalized to food intake in a group of 3 fish.
384
385 **(g)** Comparison of food intake of *oxt* null mutants (*oxt*-/-) and their heterozygous wild-type siblings (*oxt*+/-)
386 in isolated and non-isolated contexts (n = 60/59/58/54 fish). Single-group differences in food consumption
387 are abolished -- however, food intake was reduced in groups, rather than enhanced in isolated fish.
388 **p = 0.0011 (single vs group), p = 0.65 (single control vs single mutant), **p = 0.0012 (group control vs
389 group mutant), two-sided Wilcoxon rank-sum test.
390
391 **(h)** Schematic of our model for how oxytocin neurons can integrate information on social state to control
392 appetite and avoidance behaviors. We posit that social chemical cues are olfactory, and that GABAergic
393 neurons in the forebrain transform OB activation into inhibitory signals. The OXT circuit modulates
394 nocifensive behavior via brainstem premotor neurons[6]. Since it projects extensively into other parts of the
395 hypothalamus, as well as the pituitary gland, these downstream regions may be involved in mediating its
396 effects appetite[25].
397
398 Given that social isolation increases neuronal activity in a subset of OXT-positive
399 neurons and also suppresses food intake, we asked if OXT neurons are required for the social
400 control of appetite. To this end, we chemogenetically ablated OXT neurons in larvae expressing
401 bacterial-nitroreductase specifically in OXT-positive neurons, by incubation them from 5 to 7 dpf
402 (while still in a group of conspecifics) with the prodrug metronidazole (MTZ). This treatment
403 resulted in a loss of ~80% of nitroreductase-labeled preoptic OXT cells (unablated = 20.3 ± 1.1
404 neurons, ablated = 4.5 ± 0.5 neurons; n = 20 control fish, 29 fish with ablation). At 8 dpf, these

405 larvae, or MTZ-treated non-expressing controls, were then separated either into groups of 3 or
406 isolated, and assayed for feeding as described above.
407 We found that OXT neuron ablation enhanced food intake in isolated animals, while the
408 food intake of fish maintained in a group was unchanged (Fig. 4d). Consistently, addition of an
409 OXT receptor antagonist strongly increased food intake in isolated fish (Fig. 4e), whereas OXT
410 agonists strongly suppressed food intake of fish kept in a group (Fig. 4f). These results indicate
411 that OXT signaling is both necessary and sufficient to mediate the social modulation of food
412 intake observed in socially isolated fish.
413 Lastly, we compared food intake in OXT homozygous null mutant animals with their
414 heterozygous siblings. As expected, we found that null mutant animals did not modulate their
415 food intake on the basis of social environment, whereas the behavior of their heterozygous
416 siblings was indistinguishable from that of wild type animals. However, mutant animals had low
417 food intake in both the isolated and the group setting (Fig. 4g). Thus, as with acute ablation of
418 OXT neurons, social modulation of feeding was impaired. However, the generally low food
419 intake in these fish might reflect long-term deficits in circuit activity that altered the development
420 or maintenance of neural circuits involved in socially modulated behaviors. In summary, these
421 results demonstrate that, similar to nocifensive behaviors, larval zebrafish OXT neurons are
422 necessary and sufficient for social state modulation of appetite.
423
424 **DISCUSSION**
425 Larval zebrafish are generally not thought to exhibit robust social interactions, aside from simple
426 behaviors such as rudimentary avoidance of other larvae[26]. However, we found that even brief
427 (2 hr) social isolation results in distinct neural signatures that correlate with aversive and
428 nociceptive brain circuits, including activity in the preoptic area, posterior tuberculum, caudal
429 hypothalamus and, notably, populations of oxytocin (OXT)-positive neurons. This is consistent
430 with the results of a recent study (Tunbak et al, preprint online[27]) that described increased
431 activity in the preoptic area as a result of long-term social isolation in older (juvenile, 21 dpf)
432 zebrafish. Thus, in an intriguing parallel to humans[28], we note that pain and social isolation
433 exhibit a shared neural signature in the larval zebrafish brain that is likely to extend also to older
434 animals in this species.
435 Extending the analysis of the OXT-positive population revealed that these neurons are
436 functionally diverse and modulate distinct behavioral outputs, including feeding and nocifensive
437 escape responses (see also Wee et al, 2019[6]). We thus propose a circuit mechanism by which
438 the larval zebrafish integrates conspecific social cues into the modulation of defensive and

439 appetitive behaviors (Fig. 3h). Our data suggest that OXT neurons (and likely other preoptic
440 populations; Supplementary Fig. 1) encode a range of chemical social information via olfactory
441 inputs (Supplementary Fig. 2), which then becomes the basis for the modulation of nocifensive
442 and appetitive behavioral outputs. Indeed, our data reveal that the presence of conspecifics,
443 and specifically conspecific chemical cues, significantly increases appetite and reduces
444 nociceptive responses (Fig. 3 & 4). At the circuit level, OXT neurons displayed a variety of
445 responses to these chemical social cues, which could thus uniquely signal the presence of adult
446 fish (known predators), genetically-related animals (larval kin), or distantly-related (larval non-
447 kin) conspecifics. Importantly, we show that kin cues induced the most widespread inhibition of
448 OXT neurons (Fig. 2), while the same OXT neurons can be either excited or inhibited by other
449 cues, suggesting multimodal and valence-specific tuning. Notably, conspecific cues increase the
450 activity of a small subset of OXT neurons that appear to be more sensory in nature suggesting
451 that these could drive anxiolytic or anti-nociceptive effects, consistent with traditional views of
452 OXT function[3].
453 In humans and other mammals, it is known that social cues, including odors, can
454 attenuate aversive experience and behaviors, a phenomenon known as "social buffering"[20,21].
455 Social facilitation of appetite has also been observed in many species[29], and is likely
456 evolutionarily adaptive. In general, an isolated animal needs to shift its priorities from foraging to
457 vigilance or escape, since it may be more susceptible to the risk of predation. Accordingly, adult
458 zebrafish display isolation stress in a group size-dependent manner[30]. We had previously shown
459 that OXT neurons respond to a range of aversive, particularly noxious stimuli, and are sufficient
460 to drive motor responses by acting on brainstem targets[6]. By demonstrating that chemical social
461 cues converge on this circuit, and that kin cues, in particular, predominantly diminish the activity
462 of TRPA1-responsive, parvocellular OXT neurons, we provide a potential mechanistic
463 understanding of how the OXT circuit can mediate the phenomenon of "social buffering" in a
464 vertebrate organism[31].
465 Furthermore, our demonstration of a suppressive effect of OXT on appetite corroborates
466 a series of mammalian research findings: 1) The insatiable appetite and morbid obesity
467 observed in Prader Willi Syndrome is likely due to impaired OXT signaling[32,33]; 2) Acute
468 inhibition of paraventricular OXT neurons can promote food intake[34]; 3) Lesions of the PVN, as
469 well as mutations that affected OXT neuron development, have been shown to cause
470 hyperphagia and obesity[35,36], and; 4) Direct administration of OXT has been shown to reduce
471 feeding[4,5]. At the same time, our data suggests that the role of OXT in feeding may be more
472 complex than previously appreciated. Notably, while OXT homozygous mutants do not show

473 social state-dependent modulation of appetite, they also eat less than their heterozygous
474 siblings, implying that a complete absence of OXT may be detrimental towards feeding.
475 Our data further highlight the profound influence of social context on OXT's appetite-
476 suppressing effects, which may very well generalize to mammals. For example, a recent study
477 found that inhibiting OXT signaling enhances sugar intake in a socially dominant mouse
478 regardless of their social context, whereas in subordinate mice, such inhibition only enhanced
479 appetite when cues from the dominant mouse were not present[37]. Our results also complement
480 the observations of strong interactions between social and feeding circuits across evolution[38],
481 and reinforce a role for OXT in prioritizing various motivated behaviors[4]. However, effects of
482 OXT in larval zebrafish may occur as part of a coordinated response to both social isolation and
483 noxious contexts, rather than reproduction or parental care.
484 We do note some important distinctions between our findings and the canonical view of
485 OXT function as suggested by mammalian studies, the most significant of which is that the
486 larval zebrafish OXT neurons show widespread *activation* by social isolation, rather than by
487 cues indicating the presence of conspecifics[2,39]. We propose three possible reasons for these
488 apparent differences: *first*, representations within both the mammalian and zebrafish OXT
489 population are diverse and thus the observed activity patterns in zebrafish may reflect those of
490 specific subpopulations of mammalian OXT cells (indeed, some zebrafish OXT neurons are
491 activated by conspecific cues, and some mammalian OXT cells are inhibited by conspecific
492 cues[39]); *second*, OXT response properties may have changed over the course of evolution, as
493 more sophisticated social functions were derived. *Third,* there is a possibility that OXT neuron
494 response properties might reverse over the course of development, since adult and kin odor
495 generate opposite activity signatures; however, since the enhancement of preoptic area
496 activation appears to persist at least till juvenile stages (Tunbak et al, preprint online[27]), when
497 social preference behaviours have developed, any such reversal would have to happen closer
498 to adulthood. Overall, our results may provide a broader and more intricate perspective of
499 OXT's social function in vertebrate animals.
500 Furthermore, given that noxious stimuli and social isolation both activate the OXT
501 population, an enhancement of OXT signaling may in fact represent a negative valence state in
502 larval zebrafish, rather than the rewarding experience it is generally associated with.
503 Interestingly, recent studies in mammalian models have demonstrated that OXT neurons can
504 also be negatively reinforcing, and promote fear, stress and anxiety in some situations[1,40]. Thus,
505 this study could provide an evolutionary perspective on the ancient functions of this highly-
506 conserved peptide and how they relate to our current understanding of them in mammals.

In conclusion, our study demonstrates how organizing principles and circuit implementation strategies underlying social behavior can be elucidated by probing social context-dependent behaviors in a small and optically accessible model organism. More broadly, our dissection of the larval zebrafish OXT circuit provides an entrypoint into understanding how neuromodulatory systems represent behavioral states such as social isolation, hunger, and acute nociception, on multiple timescales, and how these representations are then used to modulate behavioral output in a flexible and context-dependent manner.

METHODS

Fish husbandry and transgenic lines

Larvae and adults were raised in facility water and maintained on a 14:10 hr light:dark cycle at 28°C. All protocols and procedures involving zebrafish were approved by the Harvard University/Faculty of Arts & Sciences Standing Committee on the Use of Animals in Research and Teaching (IACUC). Fish were raised at a density of ~40 fish per dish and fed from 5 dpf till the day of the experiment. Behavioral experiments were carried out mostly on fish of the WIK background, although other genotypes (e.g. AB, or mit1fa-/- (nacre) in the AB background) were also utilized and showed similar behavioral results. mit1fa-/- (nacre) in the AB background, along with additional transgenes described below, were also used for calcium imaging and MAP-mapping experiments. Transgenic lines *Tg(oxt:GFP*[41], *Tg(UAS:GCaMP6s)*[42], *Tg(UAS:nsfbCherry)*[43], *Tg(HuC:GCaMP6s)*[44], *Tg(oxt:Gal4)* and oxytocin mutants[6] were previously published.

MAP-mapping

7-8 dpf larvae, that had been continuously fed with an excess of paramecia since 5 dpf, were either isolated or split into small groups, using 35 mm dishes filled with 3 ml embryo water. For groups of 10, a larger (10 cm) dish was used to prevent overcrowding. Paramecia was present within each dish to ensure that the fish were well-fed and had ample stimulation. After 2 hrs, larvae were quickly funneled through a sieve, which was then quickly dropped into 4% paraformaldehyde, immunostained, imaged and analyzed as described in Randlett et al. (2015)[11].

Exposure to sensory cues for high-resolution pERK experiments

For generation of conspecific-conditioned water, sibling or non-sibling larvae that had been continuously fed with an excess of paramecia from 5 dpf were transferred into a new 10 cm petri dish that did not contain any paramecia, at a concentration of 2 fish per ml. After a 2 hr incubation, a syringe with an attached 0.45 µm filter was used to very gently suck out the conditioned water, with great care taken not to disturb or stress the fish in the process.

7-8 dpf larvae, that had been continuously fed with an excess of paramecia since 5 dpf, were either isolated or split into small groups, using 35 mm dishes filled with 3 ml embryo water.

547 Paramecia was present within each dish to ensure that the fish were well-fed and had ample
548 stimulation. 700 µl of the filtered conspecific-conditioned water was added to each 35 mm dish
549 (~1:5 dilution), 30 min before fixation, and embryo water was correspondingly added to controls.
550 For providing visual access to conspecifics, the 35 mm dishes containing single larvae were
551 inserted into larger (55mm) dishes containing ~5 larvae that thus be surrounding but unable to
552 interact with the single larva. After 2 hrs, larvae were quickly funneled through a sieve, which
553 was then quickly dropped into 4% paraformaldehyde, dissected in PBS and immunostained as
554 described in Wee et al, 2019[6].
555
556 *High resolution pERK analysis*
557 For quantification of pERK/tERK ratios over individual OXT neurons, pERK experiments were
558 performed on dissected *Tg(oxt:GFP)* brains. Cellular-resolution imaging of dissected brains was
559 obtained using the Zeiss (LSM 700 and LSM 880) or Olympus (FVB1000MPE) confocal
560 microscopes. pERK/tERK intensities of individual GFP-positive neurons were measured using
561 ImageJ and quantified using MATLAB as reported in Wee et al, 2019[6]. Analysis code is also
562 available on www.github.com/carolinewee

563 *Social feeding experiments*
564 For experiments in which feeding was assessed, larvae that had been continuously fed with an
565 excess of paramecia from 5 dpf were either isolated or placed in groups of 3, in 35 mm dishes
566 (3 ml embryo water), in the *absence of food*. After 2 hours, fluorescent-labeled paramecia was
567 added followed by a quick fixation after 30 min (full protocol is described in Wee et al, *eLife*,
568 2019[25]). Sensory cues were generated and presented as described above for pERK
569 experiments. Fixed larvae were subsequently distributed into 96-well flat-bottom dishes and
570 imaged using the AxioZoom V16 (Zeiss) and analyzed using Fiji software (3D Objects Counter,
571 custom software also available on www.github.com/carolinewee)
572
573 *Calcium imaging and olfactory stimulation*
574 8-11 dpf larval *Tg(oxt:Gal4;UAS:GCaMP6s)* fish in the nacre background were used for calcium
575 imaging experiments. They were embedded in the center of a 55 cm dish in 1.5% agarose with
576 their tails and noses freed.
577
578 Kin or non-kin conditioned water (at a concentration of 1 fish/ml) were generated as described
579 above. In these calcium imaging experiments, we used WIK fish as non-kin fish, since the
580 *Tg(oxt:Gal4;UAS:GCaMP6s)* fish we imaged were of the AB genetic background. For adult
581 water, 5 adult kin (from parent tank of larvae) were used to condition 500 ml of water (1 adult
582 fish/100 ml) for 2 hrs, and also subsequently filtered. Kin and non-kin fish used to condition
583 water were raised apart from experimental fish from 3 dpf, to dissociate genetic from familiarity
584 efects.
585
586 Alternating olfactory stimuli were delivered using a custom-built syringe pump system controlled
587 by custom Labview software. At specified time intervals, 300 µl of each cue (~30 µl/second) was
588 delivered using a zero-dead-volume multi-channel perfusion pencil (AutoMate Scientific).
589 Embryo water was also constantly circulated through the dish using a peristaltic pump (Harvard

590 Apparatus). The interstimulus interval (ISI) was 2 minutes for olfactory bulb imaging and 5
591 minutes for OXT neuron imaging. The longer ISI for OXT neuron imaging was implemented to
592 reduce desensitization and ensure that activity truly returned to baseline before presenting the
593 subsequent stimulus. In order to reduce experiment time and avert the possibility of OXT
594 neuron desensitization, we also never compared responses to more than 2 cues (e.g. either kin
595 vs non-kin, or kin vs adult, but not all 3 stimuli).
596
597 Calcium imaging and behavioral monitoring with TRPA1 stimulation was performed as
598 previously reported[6] on 8-10 dpf larvae, with a number of core differences: 1) 15 μM instead of
599 25 μM Optovin (Tocris Bioscienes) was used, to reduce background signals (see below) 2)
600 nostrils are exposed to allow for olfactory stimulation 3) the same UV stimulus intensity used
601 throughout the experiment, and only 4 stimulations were presented (alternating kin and water).
602 Since, in addition to the tail, the nose was exposed in this current paradigm, Optovin, a colored
603 solution, was rapidly absorbed into the fish's brain and caused a linear increase in background
604 signal (i.e. even in non-GCaMP-labeled tissue) over time. Post-hoc subtraction of this
605 background signal from OXT GCaMP signals restored a flat baseline, allowing us to extract
606 meaningful calcium signals.
607
608 *Data analysis*
609 All calcium imaging data was analyzed using custom ImageJ and MATLAB software. The
610 general protocol for analysis was: 1) Image registration to correct for motion artifacts using the
611 TurboReg[45] plugin in ImageJ; 2) Extraction of fluorescence signals from both channels using
612 manually-segmented ROIs in MATLAB or on a voxel-by-voxel basis 3) Calculation of Δf/f signals
613 from raw traces and alignment to tail traces, as needed, in MATLAB.
614
615 For fish expressing *Tg(UAS:GCaMP6s)* exclusively in oxt-expressing neurons, ROIs were
616 drawn over all visible cells in a maximum projection image for each plane and raw fluorescence
617 traces were extracted as the mean pixel value within the ROI. Other analysis was done on a
618 voxel-by-voxel basis, rather than using cell segmentation, which would exclude responses from
619 neuropil that are abundant in the OB and forebrain. Δf/f values were calculated from raw traces
620 using the average fluorescence over the time period before the first stimulus as the baseline to
621 which all traces were normalized.
622
623 Behavior, stimulation and calcium imaging timestamps were aligned and used to extract
624 stimulus-triggered averages as well as to generate motor and stimulus regressors to correlate
625 with calcium activity. The regressors were convolved with a GCaMP6s kernel based on its
626 measured response delay (0.48 s) and decay time (3s, based on Chen et al. (2013) and cross-
627 correlated with calcium traces that had been smoothed with a 3-frame zero phase filter. In order
628 to determine if an OXT neuron was activated or suppressed, we averaged the calcium signal
629 over a 60s interval post-stimulus for each stimulus type. If the difference between the two
630 integrated calcium signal during olfactory and water stimulation was more than 0.05, we
631 classified the neurons as being either activated or suppressed by the cue depending on the
632 sign. Although the threshold of 0.05 is arbitrary, we show that across a range of thresholds, the
633 relationship between the proportions of suppressed and enhanced neurons remains consistent

634 for each type of stimulus. In addition, the first stimulus was always dropped from analysis, in
635 order to account for possible effects of initial startle.
636
637 Since there was no difference in kin water responses between younger (8 dpf (n=7 fish): 35%
638 suppressed, 10% enhanced) and old (11 dpf (n = 7 fish): 37% suppressed, 10% enhanced) fish,
639 we pooled data across all the ages. Fish were isolated for between 30 min to 4 hrs before
640 imaging, though the bulk of experiments were performed with 1.5-2.5 hr isolation (note that time
641 of isolation = time of embedding). We did not observe any consistent changes in kin water
642 suppression with isolation times, thus any differences observed are likely due to random
643 variation (1 hr or less isolation (n=5): 50% suppressed, 13% enhanced; 1.5 - 2.5 hrs isolation
644 (n=19): 33% suppressed, 13% enhanced, 3-4hrs isolation (n=7): 40% suppressed, 5%
645 enhanced).
646
647 *Free-swimming TRPA1 stimulation*
648 Fish were singly placed into a 20.6 mm cut-out agarose circular mold illuminated by three quad
649 blue LEDs (Luxeon Star, 470 nm). To probe the effect of conspecific cues, DMSO or Optovin
650 solutions were generated either in embryo water or kin-conditioned water. Following 5 min of
651 habituation in DMSO (effectively also the isolation period), fish were stimulated once every 30 s
652 with a 100 ms pulse of blue light. The DMSO solution was then exchanged with Optovin, and
653 the same protocol repeated. Behavior was recorded at 200 fps (Pike F-032, Allied Vision) and
654 analyzed using custom Python software.
655
656 *Statistics*
657 All error bars show mean ± SEM over fish. Significance was reported as follows: *$p<0.05$,
658 **$p<0.01$, ***$p<0.001$. Significance was determined using the Wilcoxon signed-rank test for
659 paired data and the Wilcoxon rank-sum test for independent samples. One-sided tests were
660 used in cases where there was a clear hypothesis for the direction of effect. One-way ANOVA
661 with Bonferroni Correction was used in cases where there were multiple comparisons. Wilcoxon
662 signed rank test was used in Fig. 1a for comparing the distribution of normalized OXT ROI
663 signals across different behavioral stimuli to the null hypothesis of median 1.
664
665 **DATA AVAILABILITY**
666 All data, code (hardware control and analysis) and resources (transgenic lines/mutants
667 generated) will be made available by the corresponding author upon request.
668
669 **CODE AVAILABILITY**
670 Live versions of the analysis code are maintained at www.github.com/carolinewee.
671
672 **ACKNOWLEDGEMENTS**
673 We are grateful to Adam Douglass (Univ. of Utah) for continued support, advice, and comments.
674 We thank the CBS imaging facility, Harvard Center for Biological Imaging, and the NorthWest
675 Undergraduate Teaching Laboratories at Harvard for the successful completion of many
676 experiments. J. Miller, K. Hurley and B. Hughes provided invaluable fish care. This work was
677 supported by U01-NS090449 (FE), R24-NS086601 (FE), U19-NS104653 (FE and SK) and

Simons Foundation grant SCGB 325207 (FE). CLW was supported by the National Science Scholarship from the Agency for Science, Technology and Research (A*STAR), Singapore.

AUTHOR CONTRIBUTIONS

C.L.W., E.S., and S.K. originally conceived of the project, which was then developed into its final form with M.N and F.E.
S.K. & F.E. supervised the project. C.L.W., E.S., and M.N. designed and performed most of the experiments, and analyzed most of the data. M.N. also developed hardware and software for calcium imaging and behavioral experiments, and analyzed the free-swimming behavioral data. S.W. performed feeding experiments and analyzed data. C.L.W., S.K., and F.E. wrote the manuscript with contribution from all other authors.

COMPETING INTERESTS

The authors declare no competing interests.

REFERENCES:

1. Rash, J. A., Aguirre-Camacho, A. & Campbell, T. S. Oxytocin and pain: a systematic review and synthesis of findings. *Clin. J. Pain* **30,** 453–462 (2014).
2. Lieberwirth, C. & Wang, Z. Social bonding: regulation by neuropeptides. *Front. Neurosci.* **8,** 171 (2014).
3. Jezova, D., Skultetyova, I., Tokarev, D. I., Bakos, P. & Vigas, M. Vasopressin and Oxytocin in Stress. *Ann. N. Y. Acad. Sci.* **771,** 192–203 (1995).
4. Leng, G., Onaka, T., Caquineau, C., Sabatier, N., Tobin, V. A. & Takayanagi, Y. Oxytocin and appetite. *Prog. Brain Res.* **170,** 137–151 (2008).
5. Sabatier, N., Leng, G. & Menzies, J. Oxytocin, feeding, and satiety. *Front. Endocrinol.* **4,** 35 (2013).
6. Wee, C. L., Nikitchenko, M., Wang, W.-C., Luks-Morgan, S. J., Song, E., Gagnon, J. A., Randlett, O., Bianco, I. H., Lacoste, A. M. B., Glushenkova, E., Barrios, J. P., Schier, A. F., Kunes, S., Engert, F. & Douglass, A. D. Zebrafish oxytocin neurons drive nocifensive behavior via brainstem premotor targets. *Nat. Neurosci.* **22,** 1477–1492 (2019).
7. Lovett-Barron, M., Chen, R., Bradbury, S., Andalman, A. S., Wagle, M., Guo, S. & Deisseroth, K. Multiple overlapping hypothalamus-brainstem circuits drive rapid threat

710 avoidance. *bioRxiv* 745075 (2019). doi:10.1101/745075

711 8. Herget, U., Gutierrez-Triana, J. A., Salazar Thula, O., Knerr, B. & Ryu, S. Single-Cell
712 Reconstruction of Oxytocinergic Neurons Reveals Separate Hypophysiotropic and
713 Encephalotropic Subtypes in Larval Zebrafish. *eneuro* **4,** ENEURO.0278–16.2016 (2017).

714 9. Stoop, R. Neuromodulation by oxytocin and vasopressin. *Neuron* **76,** 142–159 (2012).

715 10. Knobloch, H. S. & Grinevich, V. Evolution of oxytocin pathways in the brain of vertebrates.
716 *Front. Behav. Neurosci.* **8,** 31 (2014).

717 11. Randlett, O., Wee, C. L., Naumann, E. A., Nnaemeka, O., Schoppik, D., Fitzgerald, J. E.,
718 Portugues, R., Lacoste, A. M. B., Riegler, C., Engert, F. & Schier, A. F. Whole-brain activity
719 mapping onto a zebrafish brain atlas. *Nat. Methods* **12,** 1039–1046 (2015).

720 12. Wircer, E., Blechman, J., Borodovsky, N., Tsoory, M., Nunes, A. R., Oliveira, R. F. &
721 Levkowitz, G. Homeodomain protein Otp affects developmental neuropeptide switching in
722 oxytocin neurons associated with a long-term effect on social behavior. *Elife* **6,** (2017).

723 13. Herget, U., Wolf, A., Wullimann, M. F. & Ryu, S. Molecular neuroanatomy and
724 chemoarchitecture of the neurosecretory preoptic-hypothalamic area in zebrafish larvae. *J.*
725 *Comp. Neurol.* **522,** 1542–1564 (2014).

726 14. Gerlach, G., Hodgins-Davis, A., Avolio, C. & Schunter, C. Kin recognition in zebrafish: a 24-
727 hour window for olfactory imprinting. *Proc. Biol. Sci.* **275,** 2165–2170 (2008).

728 15. Biechl, D., Tietje, K., Gerlach, G. & Wullimann, M. F. Crypt cells are involved in kin
729 recognition in larval zebrafish. *Sci. Rep.* **6,** 24590 (2016).

730 16. Rauch, G.-J., Granato, M. & Haffter, P. A polymorphic zebrafish line for genetic mapping
731 using SSLPs on high-percentage agarose gels. *Tech. Tips Online* **2,** 148–150 (1997).

732 17. Saito, D., Komatsuda, M. & Urano, A. Functional organization of preoptic vasotocin and
733 isotocin neurons in the brain of rainbow trout: central and neurohypophysial projections of
734 single neurons. *Neuroscience* **124,** 973–984 (2004).

735 18. Swanson, L. W. & Sawchenko, P. E. Paraventricular nucleus: a site for the integration of

736 neuroendocrine and autonomic mechanisms. *Neuroendocrinology* **31,** 410–417 (1980).
737 19. Sawchenko, P. E. & Swanson, L. W. Immunohistochemical identification of neurons in the
738 paraventricular nucleus of the hypothalamus that project to the medulla or to the spinal cord
739 in the rat. *J. Comp. Neurol.* **205,** 260–272 (1982).
740 20. Kikusui, T., Winslow, J. T. & Mori, Y. Social buffering: relief from stress and anxiety. *Philos.*
741 *Trans. R. Soc. Lond. B Biol. Sci.* **361,** 2215–2228 (2006).
742 21. Kiyokawa, Y. Social Odors: Alarm Pheromones and Social Buffering. *Curr. Top. Behav.*
743 *Neurosci.* (2015). doi:10.1007/7854_2015_406
744 22. Bazhan, N. & Zelena, D. Food-intake regulation during stress by the hypothalamo-pituitary-
745 adrenal axis. *Brain Res. Bull.* **95,** 46–53 (2013).
746 23. Shimada, Y., Hirano, M., Nishimura, Y. & Tanaka, T. A high-throughput fluorescence-based
747 assay system for appetite-regulating gene and drug screening. *PLoS One* **7,** e52549
748 (2012).
749 24. Jordi, J., Guggiana-Nilo, D., Soucy, E., Song, E. Y., Wee, C. L. & Engert, F. A high-
750 throughput assay for quantifying appetite and digestive dynamics. *Am. J. Physiol. Regul.*
751 *Integr. Comp. Physiol.* ajpregu.00225.2015 (2015). doi:10.1152/ajpregu.00225.2015
752 25. Wee, C. L., Song, E. Y., Johnson, R. E., Ailani, D., Randlett, O., Kim, J.-Y., Nikitchenko, M.,
753 Bahl, A., Yang, C.-T., Ahrens, M. B., Kawakami, K., Engert, F. & Kunes, S. A bidirectional
754 network for appetite control in larval zebrafish. *Elife* **8,** (2019).
755 26. Dreosti, E., Lopes, G., Kampff, A. R. & Wilson, S. W. Development of social behavior in
756 young zebrafish. *Front. Neural Circuits* **9,** 39 (2015).
757 27. Tunbak, H., Vazquez-Pradam, M., Ryan, T., Kampff, A. R. & Dreosti, E. The lonely fish is
758 not a loner fish: whole-brain mapping reveals abnormal activity in socially isolated
759 zebrafish. *bioRxiv* 2020.01.22.915520 (2020). doi:10.1101/2020.01.22.915520
760 28. Eisenberger, N. I., Lieberman, M. D. & Williams, K. D. Does Rejection Hurt? An fMRI Study
761 of Social Exclusion. *Science* **302,** 290–292 (2003).

762 29. Higgs, S. & Thomas, J. Social influences on eating. *Current Opinion in Behavioral Sciences*
763 **9,** 1–6 (2016).
764 30. White, L. J., Thomson, J. S., Pounder, K. C., Coleman, R. C. & Sneddon, L. U. The impact
765 of social context on behaviour and the recovery from welfare challenges in zebrafish, Danio
766 rerio. *Anim. Behav.* **132,** 189–199 (2017).
767 31. Smith, A. S. & Wang, Z. Hypothalamic oxytocin mediates social buffering of the stress
768 response. *Biol. Psychiatry* **76,** 281–288 (2014).
769 32. Swaab, D. F. Neuropeptides in hypothalamic neuronal disorders. *Int. Rev. Cytol.* **240,** 305–
770 375 (2004).
771 33. Francis, S. M., Sagar, A., Levin-Decanini, T., Liu, W., Carter, C. S. & Jacob, S. Oxytocin
772 and vasopressin systems in genetic syndromes and neurodevelopmental disorders. *Brain*
773 *Res.* **1580,** 199–218 (2014).
774 34. Atasoy, D., Betley, J. N., Su, H. H. & Sternson, S. M. Deconstruction of a neural circuit for
775 hunger. *Nature* **488,** 172–177 (2012).
776 35. Xi, D., Gandhi, N., Lai, M. & Kublaoui, B. M. Ablation of Sim1 neurons causes obesity
777 through hyperphagia and reduced energy expenditure. *PLoS One* **7,** e36453 (2012).
778 36. Tolson, K. P., Gemelli, T., Meyer, D., Yazdani, U., Kozlitina, J. & Zinn, A. R. Inducible
779 neuronal inactivation of Sim1 in adult mice causes hyperphagic obesity. *Endocrinology* **155,**
780 2436–2444 (2014).
781 37. Olszewski, P. K., Allen, K. & Levine, A. S. Effect of oxytocin receptor blockade on appetite
782 for sugar is modified by social context. *Appetite* **86,** 81–87 (2015).
783 38. Fischer, E. K. & O'Connell, L. A. Modification of feeding circuits in the evolution of social
784 behavior. *J. Exp. Biol.* **220,** 92–102 (2017).
785 39. Resendez, S. L., Namboodiri, V. M. K., Otis, J. M., Eckman, L. E. H., Rodriguez-
786 Romaguera, J., Ung, R. L., Basiri, M. L., Kosyk, O., Rossi, M. A., Dichter, G. S. & Stuber,
787 G. D. Social stimuli induce activation of oxytocin neurons within the paraventricular nucleus

788 of the hypothalamus to promote social behavior in male mice. *J. Neurosci.* (2020).
789 doi:10.1523/JNEUROSCI.1515-18.2020
790 40. Grillon, C., Krimsky, M., Charney, D. R., Vytal, K., Ernst, M. & Cornwell, B. Oxytocin
791 increases anxiety to unpredictable threat. *Mol. Psychiatry* **18,** 958–960 (2013).
792 41. Coffey, C. M., Solleveld, P. a., Fang, J., Roberts, A. K., Hong, S.-K., Dawid, I. B.,
793 Laverriere, C. E. & Glasgow, E. Novel oxytocin gene expression in the hindbrain is induced
794 by alcohol exposure: transgenic zebrafish enable visualization of sensitive neurons. *PLoS*
795 *One* **8,** e53991 (2013).
796 42. Muto, A., Lal, P., Ailani, D., Abe, G., Itoh, M. & Kawakami, K. Activation of the hypothalamic
797 feeding centre upon visual prey detection. *Nat. Commun.* **8,** 15029 (2017).
798 43. Davison, J. M., Akitake, C. M., Goll, M. G., Rhee, J. M., Gosse, N., Baier, H., Halpern, M.
799 E., Leach, S. D. & Parsons, M. J. Transactivation from Gal4-VP16 transgenic insertions for
800 tissue-specific cell labeling and ablation in zebrafish. *Dev. Biol.* **304,** 811–824 (2007).
801 44. Kim, D. H., Kim, J., Marques, J. C., Grama, A., Hildebrand, D. G. C., Gu, W., Li, J. M. &
802 Robson, D. N. Pan-neuronal calcium imaging with cellular resolution in freely swimming
803 zebrafish. *Nat. Methods* **14,** 1107–1114 (2017).
804 45. Thevenaz, P., Ruttimann, U. E. & Unser, M. A pyramid approach to subpixel registration
805 based on intensity. *IEEE Trans. Image Process.* **7,** 27–41 (1998).

806